ARTICLE
Journal of Cellular Biochemistry 107:1129–1138 (2009)

Journal of Cellular Biochemistry

The Immunoglobulin-Like Cell Adhesion Molecule HepaCAM Induces Differentiation of Human Glioblastoma U373-MG Cells

Lay Hoon Lee, Mei Chung Moh, Ting Zhang, and Shali Shen*

Department of Physiology, Yong Loo Lin School of Medicine, National University of Singapore, 2 Medical Drive, Singapore 117597, Singapore

ABSTRACT

Subsequent to our identification of a novel immunoglobulin-like cell adhesion molecule hepaCAM, we showed that hepaCAM is frequently lost in diverse human cancers and is capable of modulating cell motility and growth when re-expressed. Very recently, a molecule identical to hepaCAM (designated as GlialCAM) was found highly expressed in glial cells of the brain. Here, we demonstrate that hepaCAM is capable of inducing differentiation of the human glioblastoma U373-MG cells. Expression of hepaCAM resulted in a significant increase in the astrocyte differentiation marker glial fibrillary acid protein (GFAP), indicating that hepaCAM promotes glioblastoma cells to undergo differentiation. To determine the relationship between hepaCAM expression level and cell differentiation, we established two U373-MG cell lines expressing hepaCAM at different levels. The results revealed that high-level hepaCAM triggered a clear increase in GFAP expression as well as morphological changes characteristic of glioblastoma cell differentiation. Furthermore, high expression of hepaCAM significantly accelerated cell adhesion but inhibited cell proliferation and migration. Concomitantly, deregulation of cell cycle regulatory proteins was detected. Expectedly, the differentiation was noticeably less apparent in cells expressing low-level hepaCAM. Taken together, our findings suggest that hepaCAM induces differentiation of the glioblastoma U373-MG cells. The degree of cell differentiation is dependent on the expression level of hepaCAM. J. Cell. Biochem. 107: 1129–1138, 2009.

KEY WORDS: HEPACAM; IMMUNOGLOBULIN-LIKE CELL ADHESION MOLECULE; DIFFERENTIATION; GLIOBLASTOMA U373-MG; GLIALCAM

Astrocytes are the major glial cells in the central nervous system (CNS). These non-neuronal cells are differentiated from neural stem cells within the ventricular and subventricular zone of developing CNS [Levison and Goldman, 1993; Barres, 1999; Mi et al., 2001; Pringle et al., 2003]. Astrocytes play important roles in the development and function of the CNS. Besides providing support and nutrition to neurons, they are involved in maintaining brain homeostasis, re-recycling neurotransmitters, and modulating synaptic transmission. Genetic alterations of astrocyte differentiation-associated genes may predispose the cells or their precursors to undergo malignant transformation, giving rise to astrocytomas [Ferreira and Kosik, 1996; Adachi et al., 1999; Kim et al., 2004; Bleau and Holland, 2007]. Astrocytomas are the most common malignancy of the CNS, accounting for >60% of primary brain tumors [DeAngelis, 2001]. The most aggressive form of astrocytoma is glioblastoma. Glioblastoma cells, composed of poorly differentiated neoplastic astrocytes, share similar characteristics with the normal neural precursor cells including rapid cell proliferation, migration, and invasion [Collins, 1998; Rasheed et al., 1999; Sasaki et al., 2002]. Despite progresses made in the treatment of glioblastoma, the overall prognosis remains extremely poor with a median survival of about 12 months [Krex et al., 2007]. Understanding the genetic events that regulate astrocyte differentiation may contribute to the development of new therapeutic targets for astrocytoma treatment.

Cell adhesion molecules are transmembrane receptors that mediate cell–extracellular matrix and cell–cell interactions fundamental for many biological processes such as differentiation [Gumbiner, 1996; Bischoff, 1997; Cavenagh et al., 1998]. Previously, we reported the identification of a novel gene *hepaCAM* in liver that encodes a cell adhesion molecule of the immunoglobulin superfamily [Moh et al., 2005a]. The hepaCAM protein

Lay Hoon Lee and Mei Chung Moh contributed equally to this work.

Grant sponsor: National University of Singapore Academic Research Fund Grant; Grant numbers: R-185-000-112-112, R-185-000-169-112; Grant sponsor: Singapore Millennium Foundation Postdoctoral Fellowship Grant.

*Correspondence to: Dr. Shali Shen, Department of Physiology, Yong Loo Lin School of Medicine, National University of Singapore, 2 Medical Drive, Singapore 117597, Singapore. E-mail: phsssl@nus.edu.sg

Received 10 February 2009; Accepted 22 April 2009 • DOI 10.1002/jcb.22215 • © 2009 Wiley-Liss, Inc.
Published online 8 June 2009 in Wiley InterScience (www.interscience.wiley.com).

contains an extracellular domain consisting of two immunoglobulin loops, a transmembrane segment and a cytoplasmic tail. We have demonstrated that hepaCAM is glycosylated and phosphorylated, and forms *cis*-homodimer on cell surface. The gene is found to be ubiquitously expressed in normal liver tissues but frequently downregulated in human hepatocellular carcinoma (HCC). Overexpression of hepaCAM in HepG2, a hepaCAM-deficient HCC cell line, significantly inhibits cell colony formation and delays cell growth, suggesting a role of hepaCAM in tumor suppression. Furthermore, expression of hepaCAM promotes cell–extracellular matrix adhesion and cell motility [Moh et al., 2005a,b]. In a recent report, we show that *hepaCAM* is widely expressed in the human tissues and is frequently silenced in a variety of tumor types [Moh et al., 2008].

According to the gene expression data from GeneNote (GeneCard database, www.genecards.org), *hepaCAM* is most highly expressed in the brain and spinal cord of normal human CNS. Consistently, Favre-Kontula et al. [2008] have recently isolated a protein identical to hepaCAM designated as GlialCAM from the human brain. They show that GlialCAM is predominantly expressed in human and mouse CNS, particularly in the glia-rich regions of brain and spinal cord. A possible role for GlialCAM in myelination is supported by its temporal upregulated expression during postnatal mouse CNS development, corresponding with the expression levels of myelin basic protein. In vitro studies on rat-derived cells demonstrate that GlialCAM is expressed in different stages of oligodendrocyte differentiation as well as in the processes of bipolar astrocytes, implying an involvement of the protein in glial cell differentiation. However, it remains unclear if hepaCAM could indeed induce differentiation of glial cells. In this present work, using the human glioblastoma U373-MG cell line as a model, we investigated the relationship between hepaCAM and astrocytic differentiation, and determined the effect of hepaCAM expression level on differentiation. The cells were transfected with hepaCAM; and the morphological changes, glial fibrillary acid protein (GFAP) expression, as well as the growth, adhesive, and invasive properties of the transfectants were assessed.

MATERIALS AND METHODS

CELL CULTURE, PLASMID, TRANSFECTION, AND COLONY FORMATION

Human glioblastoma U373-MG (a gift from Dr. Celestial Yap) and HCC C3A cells (American Type Culture Collection, Manassas, VA) were cultured in 10% fetal bovine serum (FBS; Life Technologies, Gaithersburg, MD)-supplemented Dulbecco's modified Eagle's medium nutrient mixture F-12 (DMEM/F12; HyClone Laboratories, Logan, UT) and DMEM (Sigma, St. Louis, MO), respectively. The construction of V5-tagged hepaCAM plasmid (hepaCAM-V5; hepaCAM cDNA cloned into pcDNA6/V5-His vector) was previously described [Moh et al., 2005a]. Transient and stable transfections were carried out using the reagent of Lipofectamine Plus (Invitrogen, Carlsbad, CA) according to the manufacturer's instructions. Cells were harvested 48 h after transient transfection. Stable U373-MG cell lines were established by selection in 10 μg/ml of blasticidin (Invitrogen) for 2 weeks and then cloned. For colony formation, parental or stable clones of transfected U373-MG (3×10^4) cells were seeded into 100-mm plates and cultured for 2 weeks. The colonies formed at the end of the experiment were stained with 1% crystal violet.

RNA ISOLATION AND SEMI-QUANTITATIVE REVERSE TRANSCRIPTION-POLYMERASE CHAIN REACTION (RT-PCR)

Total RNA from cultured cells was extracted with the RNeasy kit (Qiagen, Hilden, Germany) and treated with DNase (Qiagen) to digest contaminating DNA. RT-PCR reactions were performed using the OneStep RT-PCR kit (Qiagen). A forward primer (5′-tgtacagctg-catggtggaga-3′) and a reverse primer (5′-tctggtttcaggcggtcatca-3′) were used to generate a hepaCAM fragment of 235 bp from 0.2 mg of DNase-treated total RNA. Glyceraldehyde 3-phosphate dehydrogenase (GAPDH) served as a loading control. RT-PCR products were analyzed by gel electrophoresis.

GROWTH CURVE

The growth rate of parental U373-MG cells or stable U373-MG clones expressing pcDNA6/V5-His vector or hepaCAM-V5 was monitored for 6 days. Cells were seeded in 6-well plates and cultured under standard conditions. At every 24 h, cell viability was evaluated by microtetrazolium (MTT) assay. The growth rate of each cell line was presented as fold of increase in cell viability against the respective base line obtained on the day of seeding cells.

FLOW CYTOMETRY

For cell cycle analysis, cells fixed in 70% ethanol were resuspended in staining solution (200 μg/ml propidium iodide, 0.1% Triton X-100, and 2 mg/ml RNase A) and incubated for 15 min at 37°C. The distribution of cells was determined using the Beckman Coulter Epics Altra flow cytometer (Krefeld, Germany). Data were analyzed using WinMDI software version 2.8.

PROTEIN EXTRACTION AND WESTERN BLOT ANALYSIS

Cells were lysed in radioimmunoprecipitation assay buffer supplemented with protease inhibitors. Protein lysates were resolved by sodium dodecyl sulfate (SDS) polyacrylamide gel electrophoresis and transferred to polyvinylidene difluoride membranes (Biorad, Richmond, CA). Mouse anti-hepaCAM (R&DSystems, Minneapolis, MN) and anti-V5 (Invitrogen) antibodies were used to detect endogenously- and exogenously expressed hepaCAM, respectively. Antibodies against GFAP, p21, cyclin D1, cyclin B1, and GAPDH were purchased from Santa Cruz Biotechnology (Santa Cruz, CA). Proteins were detected with the appropriate horseradish peroxidase-conjugated secondary antibody followed by development with chemiluminescence luminol reagent (Santa Cruz Biotechnology) and autoradiography. The intensity of bands was quantified with a GS-800 densitometer and QuantityOne software (Biorad).

IMMUNOFLUORESCENCE

Cells cultured in 4-well chamber slides (Nunc, Naperville, IL) were fixed with 3.7% paraformaldehyde and permeabilized with 0.2% Triton X-100. Protein expression of hepaCAM-V5 was detected using rabbit anti-V5 antibody (Bethyl Laboratories, Montgomery, TX), followed by Alexa Fluor 488 goat anti-rabbit

IgG antibody (Molecular Probes, Eugene, OR). For colocalization studies, GFAP protein was detected using mouse anti-GFAP antibody, biotin-conjugated goat anti-mouse IgG antibody (Santa Cruz Biotechnology), and subsequently avidin–tetramethylrhodamine isothiocyanate conjugate (Sigma). Cell fluorescence was visualized by fluorescence microscopy.

WOUND HEALING ASSAY

Cells grown to confluence in 6-well culture plates were scratched with a sterile plastic 200-μl micropipette tip. The wounds were viewed under a light microscope immediately after wounding and representative wound sites were marked on the culture plates. The marked areas were observed at the indicated time and photographed. The percentage of wound closure was calculated by measuring the remaining gap space on the pictures.

TRANSWELL INVASION ASSAY

Cell invasion was assessed using transwell chambers with 8-μm pore size membranes (Costar, Cambridge, MA) coated with matrigel (BD Biosciences, Bedford, MA) in 24-well plates. The cells were starved overnight in serum-free DMEM/F12 medium containing 0.1% bovine serum albumin prior to initiation of assay. Cells (5×10^4) resuspended in DMEM/F12 containing 1% FBS were added into the upper chamber of a transwell and allowed to migrate through the membrane for 72 h. Non-migrated cells on the upper side of the membrane were removed with a cotton swab. The migrated cells were stained with 1% crystal violet. The crystal violet stain was dissolved in 0.1% SDS solution and quantified by absorbance at 595 nm.

CELL SPREADING ASSAY

Cells were seeded in plates coated with 10 μg/ml fibronectin (Sigma) and incubated under standard culture conditions. Unspread cells were defined as round cells, while spread cells were defined as cells with extended processes [Richardson et al., 1997]. The number of spread cells was counted in five randomly selected microscopic fields at the indicated time points and presented as a percentage of total cells counted.

STATISTICAL ANALYSIS

All statistical analyses were performed with the software InStat 3.0 (GraphPad, San Diego, CA). Analysis of variance (ANOVA) test was performed to compare the differences among more than two means. $P < 0.05$ was considered significant.

RESULTS

INDUCTION OF GFAP EXPRESSION IN U373-MG CELLS BY HEPACAM

To determine the expression of hepaCAM in U373-MG cells, RT-PCR and Western blot analysis were performed. The result showed that neither hepaCAM mRNA nor protein (Fig. 1A) was detected in the cells, indicating that hepaCAM is lost at the transcriptional level in U373-MG cells.

The hepaCAM-deficient U373-MG cells were subsequently transfected with hepaCAM-V5 plasmid to investigate if the molecule

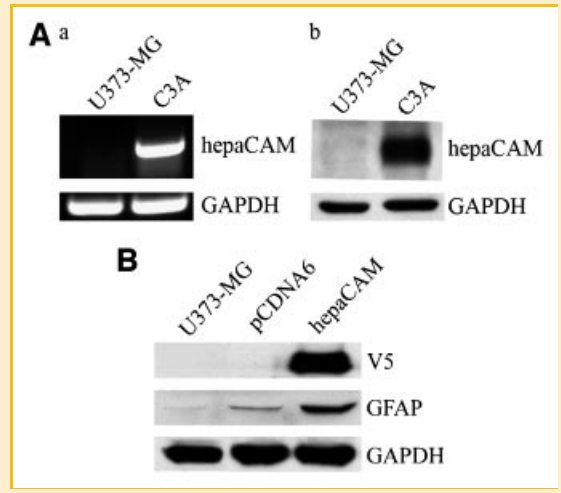

Fig. 1. Induction of GFAP expression by hepaCAM in U373-MG cells. A: Evaluation of hepaCAM expression in U373-MG cells. a: Semi-quantitative RT-PCR products were analyzed by gel electrophoresis. b: Western blot analysis of hepaCAM expression using anti-hepaCAM antibody. C3A cells served as the positive control. GAPDH was included as the loading control. B: U373-MG cells were transiently transfected with hepaCAM-V5 plasmid (hepaCAM) or pcDNA6/His-V5 vector (pcDNA6). Fifty micrograms of cell lysates prepared from parental and transfected cells was subjected to Western blot analysis using antibodies against V5 (to detect hepaCAM), GFAP, and GAPDH (loading control).

was capable of inducing differentiation of the glioblastoma cells by assessing GFAP expression. GFAP is a reliable marker of differentiated astrocytes. In comparison to parental and pcDNA6/His-V5 vector-transfected cells, transient expression of hepaCAM resulted in an elevated expression of GFAP protein (Fig. 1B). The increased expression of GFAP in the hepaCAM-transfected cells suggests an association of hepaCAM with differentiation.

ESTABLISHMENT OF STABLE U373-MG CLONAL CELL LINES

To further study the functional role of hepaCAM in glioblastoma, we stably transfected U373-MG cells with either pcDNA6/His-V5 vector or hepaCAM-V5 plasmid. The cells were then cloned after 2 weeks of antibiotic selection. A clone transfected with vector (V1) and two clones expressing hepaCAM (hCAM1 and hCAM2) were selected for downstream functional analyses. Western blot analysis using anti-V5 antibody verified that hepaCAM-V5 was absent in both parental and V1 cells, but expressed in hCAM1 and hCAM2 cells (Fig. 2A). hCAM1 and hCAM2 cells expressed hepaCAM at different levels. The level of hepaCAM expression in hCAM2 cells was approximately fourfold higher than in hCAM1 cells (Fig. 2B). Immunofluorescence staining confirmed the homogeneity of the cell clones established and the expression levels of hepaCAM in hCAM1 and hCAM2 cells (Fig. 2C). In addition, the data showed the hepaCAM protein was localized predominantly on the plasma membrane of U373-MG cells.

INCREASED GFAP EXPRESSION IN STABLE U373-MG CLONES EXPRESSING HEPACAM

The results in Fig. 1B showed that hepaCAM induced the expression of GFAP. To verify the expression of GFAP in the stable clones,

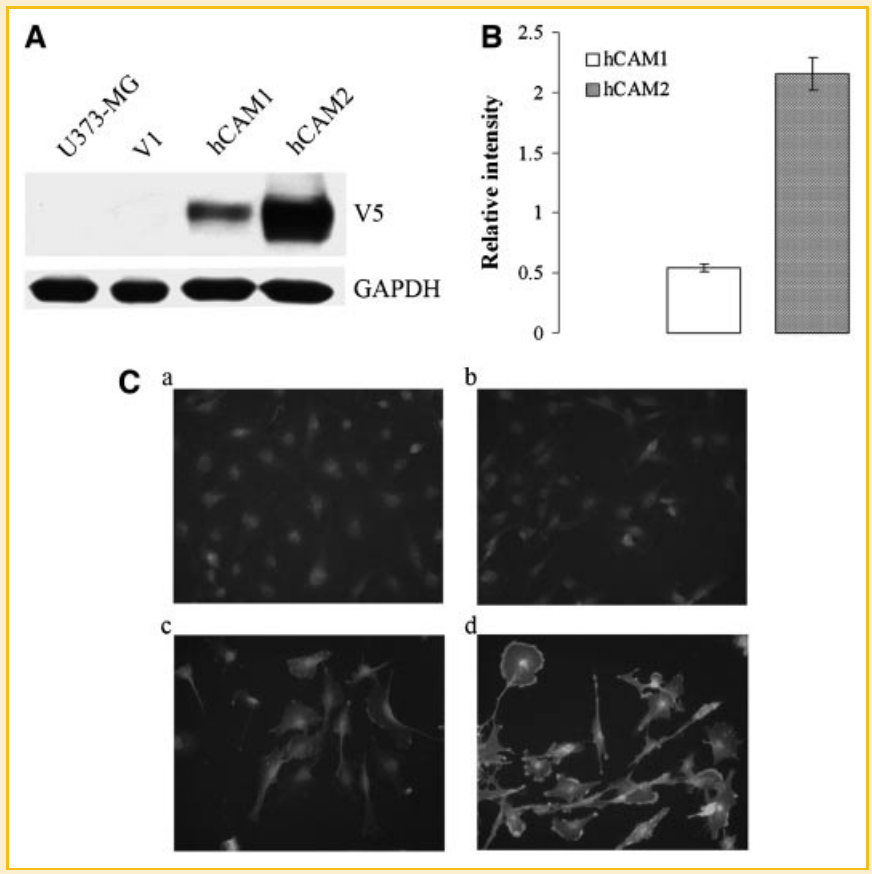

Fig. 2. Establishment of stable U373-MG clones. U373-MG cells stably transfected with pcDNA6/His-V5 vector or hepaCAM-V5 plasmid were cloned. One clone transfected with vector (V1) and two clones expressing different levels of hepaCAM (hCAM1 and hCAM2) were selected for functional studies. A: Western blot analysis to detect hepaCAM expression in parental cells and stable clones using anti-V5 antibody. GAPDH was included as loading control. B: Bar graph depicting the relative intensity of hepaCAM expression in hCAM1 and hCAM2 cells. Protein band intensities were measured and the values were normalized against GAPDH. Data represent means ± SD of three independent experiments. C: Cellular localization of hepaCAM protein in (a) parental, (b) V1, (c) hCAM1, and (d) hCAM2 cells (cultured for 1 week) by indirect immunofluorescence with rabbit anti-V5 antibody. Microscopic photos were taken at 320× magnification.

Western blot was performed. The expression of GFAP was indeed increased in hCAM1 ($P < 0.01$) and hCAM2 ($P < 0.001$) cells as compared to parental and V1 cells (Fig. 3A,B). Expectedly, the level of GFAP in hCAM2 cells was about fourfold higher than in hCAM1 cells (Fig. 3B). This finding suggests that the expression of GFAP correlates with the expression of hepaCAM.

Immunofluorescence analysis of the stable cells showed that the intensity of GFAP staining appeared stronger in hCAM2 cells than in hCAM1 cells (Fig. 3C), re-affirming the Western blot result shown in Figure 3A. In addition, colocalization of hepaCAM and GFAP was clearly observed in hCAM2 cells. The proteins prominently colocalized in a scattered pattern along the plasma membrane, particularly at the tips of cell protrusions.

MORPHOLOGICAL CHANGES OF STABLE U373-MG CLONES EXPRESSING HEPACAM

Differentiation of astrocytoma cells is characterized by morphological changes from a polygonal morphology to spindle shape with processes [Li et al., 2007]. Microscopic examination of the parental cells and stable clones revealed that V1 cells had a polygonal morphology similar to that of parental U373-MG cells (Fig. 4). In contrast, most of hCAM1 cells became elongated but without extended processes. hCAM2 cells, on the other hand, displayed small cell bodies with long, thin processes. Moreover, many of hCAM2 cells appeared bipolar. The result indicates that while cells of hCAM1 are undergoing differentiation, the cells of hCAM2 may have entered a differentiated state.

GROWTH INHIBITION OF STABLE U373-MG CLONES EXPRESSING HEPACAM

The growth rate of parental cells and stable clones was monitored for a 6-day period and evaluated by MTT assay (Fig. 5A). When compared with the growth rate of parental cells on day 6, the growth of V1 cells was ~20% faster, while hCAM1 and hCAM2 cells were ~29% and ~48% slower, respectively. The result was verified by colony formation assay (Fig. 5B). We then examined the expression of G1 and G2/M cell cycle regulatory proteins including p21, cyclin D1, and cyclin B1 in these cells (Fig. 6). In comparison to parental and V1 cells, the expression of p21 ($P < 0.001$) was upregulated while cyclins D1 ($P < 0.001$) and B1 ($P < 0.001$) were

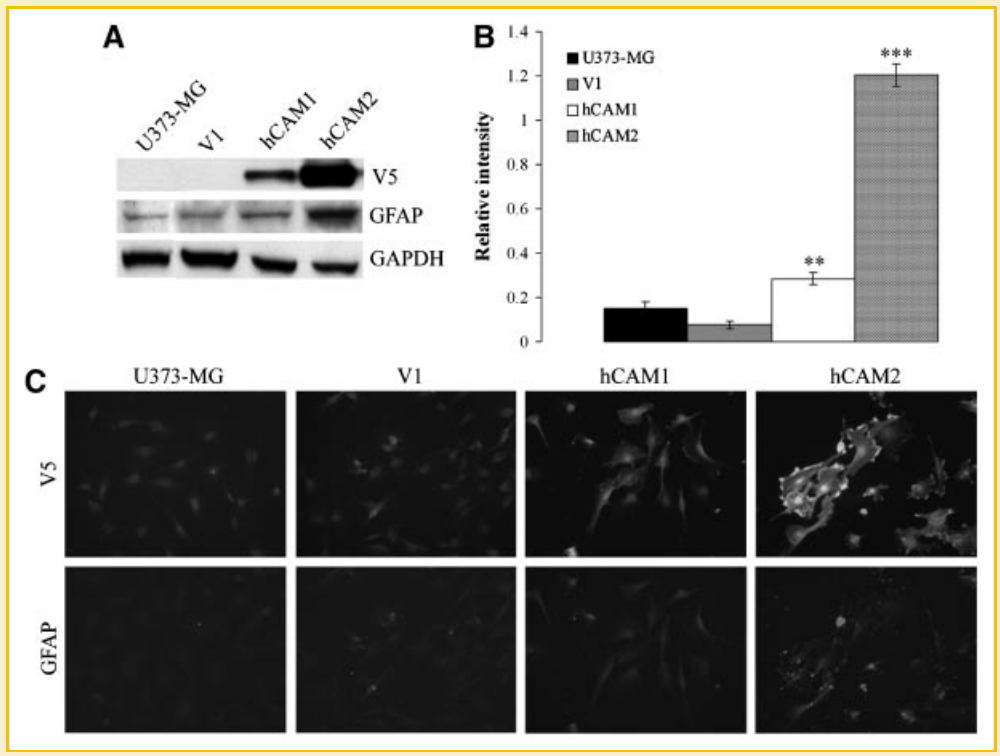

Fig. 3. Expression of GFAP in stable U373-MG clones. A: Fifty micrograms of cell lysates prepared from parental cells and stable clones was subjected to Western blot analysis using antibodies against V5, GFAP, and GAPDH (loading control). B: Bar graph depicting the relative intensity of GFAP expression. Protein band intensities were measured and the values were normalized against GAPDH. Data represent means ± SD of three independent experiments. $^{**}P < 0.01$, $^{***}P < 0.001$ as assessed by ANOVA test. C: Colocalization analysis of GFAP and hepaCAM. Parental cells and stable clones (cultured for 1 week) were double-labeled with rabbit anti-V5 antibody and mouse anti-GFAP antibody. Fluorescence was visualized by fluorescence microscopy. Microscopic photos were taken at 320× magnification.

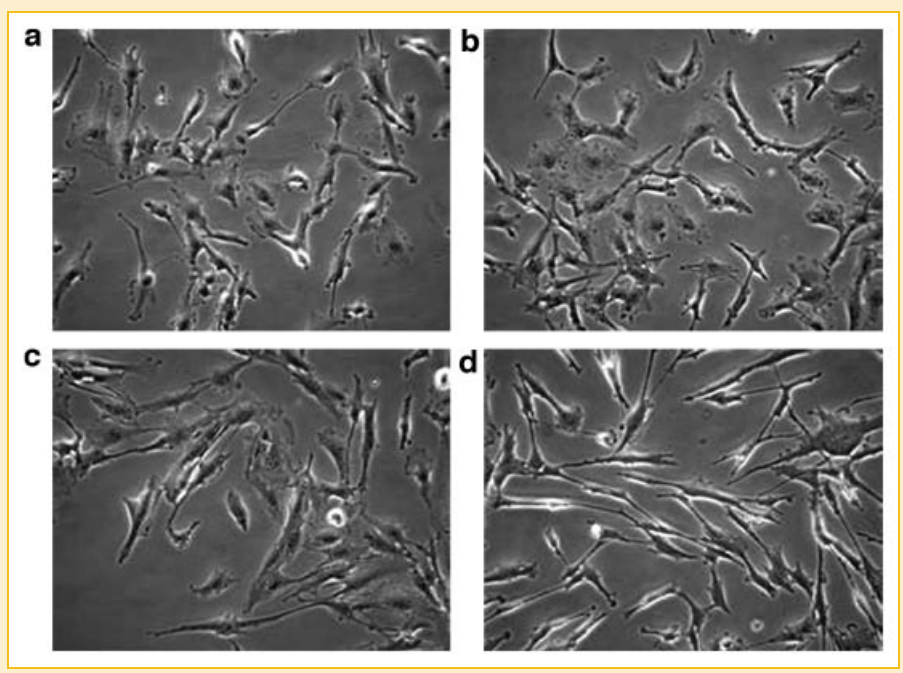

Fig. 4. Cell morphology of stable U373-MG clones. The morphology of (a) parental, (b) V1, (c) hCAM1, and (d) hCAM2 cells (cultured for 4 weeks) was observed microscopically and photographed at 320× magnification.

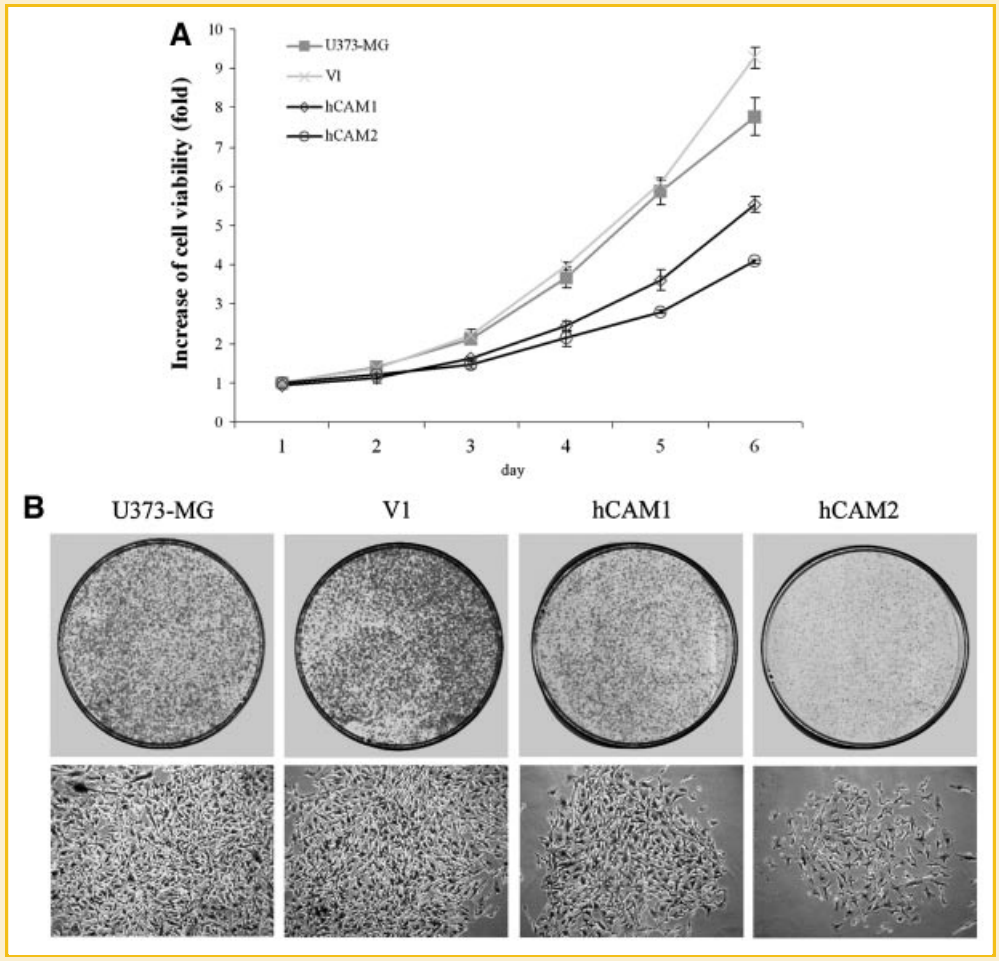

Fig. 5. Cell growth analysis of stable U373-MG clones. A: Growth curve. The growth rate of parental cells and stable clones was assessed for 6 days by MTT assay. Data represent means ± SD of three independent experiments. B: Colony formation. Parental cells and stable clones were seeded and cultured for 2 weeks. The colonies formed at the end of the experiment were stained with 1% crystal violet (top panel). Microscopic photos of the average cell density in a crystal violet-stained colony were taken at 100× magnification (bottom panel). One of the three representative experiments is shown.

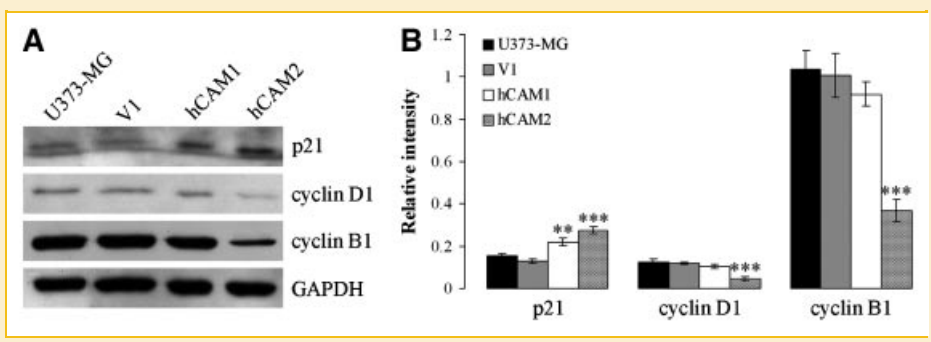

Fig. 6. Expression of cell cycle regulatory proteins in stable U373-MG clones. A: Fifty micrograms of cell lysates prepared from parental cells and stable clones was subjected to Western blot analysis using antibodies against p21, cyclin D1, cyclin B1, and GAPDH (loading control). B: Bar graph depicting relative expression of the cell cycle regulatory proteins. Protein band intensities were measured and the values were normalized against GAPDH. Data represent means ± SD of three independent experiments. $^{**}P < 0.01$, $^{***}P < 0.001$ as assessed by ANOVA test.

downregulated in hCAM2 cells. hCAM1 cells had an elevated expression of p21 ($P < 0.01$) but no clear reduction of cyclins D1 and B1. Although cell proliferation was suppressed in hCAM1 and hCAM2 cells, cell cycle analysis showed that hepaCAM had no significant effect ($P > 0.05$) on cell cycle progression, that is, the population of hCAM1 and hCAM2 cells distributed in each phase of the cell cycle was similar to that of the control cells (Fig. 7). The results suggest that hepaCAM is capable of inhibiting cell growth without affecting the cell cycle profile.

INCREASED CELL ADHESION OF STABLE U373-MG CLONES EXPRESSING HEPACAM

The adhesive role of hepaCAM was examined using the cell spreading assay. The parental cells and stable clones were allowed to spread on fibronectin-coated substrates. The result in Figure 8A showed that cells of hCAM1 ($P < 0.001$) and hCAM2 ($P < 0.001$) spread faster on fibronectin as compared to those of parental and V1 at both 30- and 60-min time points. Clearly, when expressed at high level, hepaCAM induced a higher percentage of cells to spread than at low level ($P < 0.001$). No significant difference in the adhesion rate of parental and V1 cells was detected.

EVALUATION OF MIGRATION POTENTIAL OF STABLE U373-MG CLONES

Cell migration was assessed by wound healing and transwell invasion assays. For wound healing assay, confluent monolayers of parental cells and stable clones were scratched and allowed to heal. Cells were observed at the indicated time points. As shown in Figure 8B, while the rate of wound healing was slowest in hCAM2 cells ($P < 0.001$), the wound closure rate of parental, V1, and hCAM1 cells was comparable. Similarly in transwell invasion assay, hCAM2 cells ($P < 0.05$) had the least number of migrated cells as compared to parental, V1, and hCAM1 cells (Fig. 8C). Together, the results suggest that a high expression level of hepaCAM is required for inhibiting cell migration.

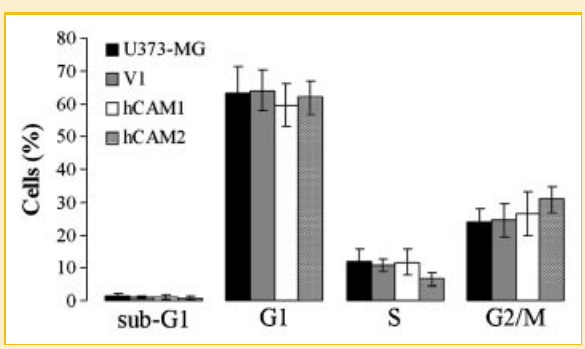

Fig. 7. Cell cycle profile of stable U373-MG clones. The cell cycle distribution of parental cells and stable clones was analyzed by flow cytometry. Bar graph representing the percentage of cells in each phase of the cell cycle. Data represent means ± SD of three independent experiments. $P > 0.05$ as assessed by ANOVA test.

DISCUSSION

Subsequent to our identification of the immunoglobulin-like cell adhesion molecule hepaCAM in the human liver [Moh et al., 2005a], Favre-Kontula et al. [2008] reported the isolation of a protein identical to hepaCAM from the CNS. Designated as GlialCAM, the protein has been found to be highly expressed in normal human and mouse CNS, particularly in the regions that are rich in glial cells. The observation of upregulated expression of GlialCAM during postnatal mouse brain development together with the detection of GlialCAM expression at different stages of oligodendrocyte differentiation and in primary astrocytes implies a potential role of the molecule in glial cell differentiation. Differentiated astrocytes are characterized by increased GFAP expression, a change from polygonal to spindle-shaped morphology, and inhibited cell proliferation and motility [Bovolenta et al., 1984; Hatten, 1984; Hatton and Hoi, 1993; Li et al., 2007]. In this work, we provide experimental evidence to show that expression of hepaCAM induces differentiation of the poorly differentiated glioblastoma U373-MG cell line.

Controlled regulation of differentiation is critical for normal development and homeostasis [Raff, 1996]. Loss of differentiation in malignant tumors has been associated with aberrant gene expression [Ferreira and Kosik, 1996; Adachi et al., 1999; Kim et al., 2004; Bleau and Holland, 2007]. To date, no studies on the expression profile of hepaCAM in normal and malignant CNS tissues in relation to differentiation have been reported. However, the predominant expression of GlialCAM in the glia-rich areas of normal brain [Favre-Kontula et al., 2008] and the absence of hepaCAM in U373-MG cells and another glioblastoma cell line Hs683 [Moh et al., 2008] may preliminarily suggest that *hepaCAM* is differentially expressed in tumors of glial cells. Nevertheless, it is worth evaluating cell lines and tissues to determine the expression pattern of *hepaCAM* during astrocytoma development and progression. If *hepaCAM* indeed participates in astrocytic differentiation, silencing of the gene in astrocytes may disrupt the intrinsic differentiation signaling, which in turn, lead to the development and malignant transformation of astrocytomas.

To study differentiation, we examine the expression of GFAP, a reliable marker of astrocyte differentiation. GFAP protein is expressed exclusively in astrocytes of the CNS and its expression level increases with the degree of astrocytic differentiation [Dahl, 1981; Bovolenta et al., 1984]. Transfection studies were employed in this investigation because expression of gene *hepaCAM* is completely lost in U373-MG cells. Re-expression of hepaCAM in U373-MG cells results in an upregulated expression of GFAP. In addition, when stably expressed, hepaCAM changes the cell morphology, suppresses cell growth, and reduces the migration capacity of the U373-MG cells. Furthermore, hepaCAM promotes the adhesion of the cells to the extracellular matrix component fibronectin. It is accepted that cell–matrix adhesion plays an important role in regulating differentiation. Studies have shown that inhibition of extracellular matrix synthesis [Nandan et al., 1990; Saitoh et al., 1992] as well as blockage of integrin function [Menko and Boettiger, 1987] inhibits the differentiation of myoblasts. Moreover, myoblasts in suspension fail to differentiate in the

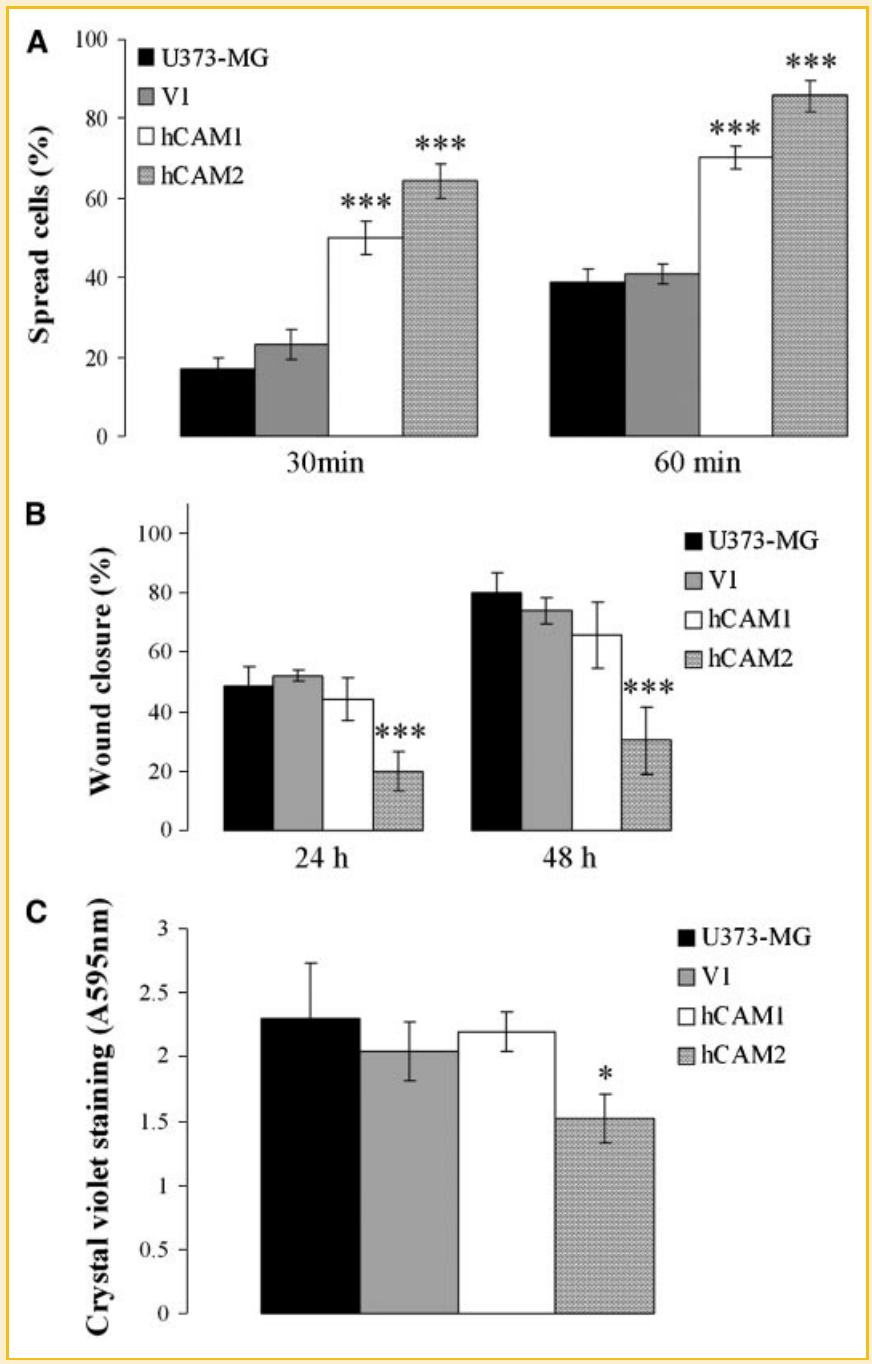

Fig. 8. Adhesion and migration potential of stable U373-MG clones. A: Cell spreading assay. Cells were allowed to spread on fibronectin-coated plates for 30 and 60 min. At the indicated time points, the number of spread cells was counted in five randomly selected microscopic fields. Bar graph depicts the mean percentage of spread cells. Data shown are means ± SD (n = 5). $^{***}P < 0.001$ as assessed by ANOVA test. B: Wound healing assay. Confluent monolayers of parental cells and stable clones were scratched by a pipette tip. The diameters of wounds were measured at 0, 24, and 48 h after wounding. Bar graph representing the percentage of wound closure. Data shown are means ± SD (n = 6) from one of the three representative experiments. $^{***}P < 0.001$ as assessed by ANOVA test. C: Transwell invasion assay. Parental cells and stable clones were seeded in the upper chamber of Matrigel-coated transwell inserts and allowed to migrate. After 72 h of incubation, the migrated cells were stained with 1% crystal violet. The crystal violet stain of the cells was dissolved in 0.1% SDS solution and quantified by absorbance at 595 nm. Bar graph depicting the absorbance of dissolved crystal violet. Data shown are means ± SD (n = 5) from one of the three representative experiments. $^{*}P < 0.05$ as assessed by ANOVA test.

absence of substrate adhesion [Milasincic et al., 1996]. Leventhal and Feldman [1996] also demonstrated that increased tyrosine phosphorylation of the focal adhesion protein paxillin in neuronal cells leads to cell spreading and neurite outgrowth typical of a differentiated neuronal phenotype. Together, our findings support the role of hepaCAM in glioblastoma cell differentiation.

Interestingly, the extent of differentiation of U373-MG correlates with the levels of hepaCAM expression. The stable cells expressing

high level of hepaCAM exhibit stronger differentiation phenotypes than cells expressing low-level hepaCAM. The results demonstrate that high-level hepaCAM expression triggers a clear increase in GFAP expression as compared to low-level hepaCAM expression. Moreover, cells with high expression of hepaCAM display distinct morphological changes typical of differentiated astrocytes. On the contrary, changes in morphology are less discrete in the cells with low expression level of hepaCAM. Furthermore, the rate of cell proliferation is markedly slower in cells expressing high level of hepaCAM. The adhesive rate of cells is faster when hepaCAM is expressed at high level. While cells expressing high-level hepaCAM display reduced migration capacity, cells with low-level hepaCAM have a migration rate similar to that of the control cells. Overall, the results suggest that the degree of astrocytic differentiation is dependent on the expression level of hepaCAM.

We have previously shown that overexpression of hepaCAM in both HCC HepG2 cells [Moh et al., 2005a] and breast cancer MCF7 cells [Moh et al., 2005b] promotes cell migration. Intriguingly, introduction of hepaCAM into U373-MG cells inhibits cell motility and invasion. Although the exact mechanism of hepaCAM-induced migration has not been defined, it is conceivable that the molecule signals through various pathways to promote and inhibit cell migration in different cell types.

Expression of hepaCAM inhibits cell growth and colony formation of transfected U373-MG cells. Analysis of the effect of hepaCAM on the expression of cell cycle regulatory proteins has revealed that high-level hepaCAM increases the protein level of p21 and decreases cyclins D1 and B1. Cyclin D1 [Sherr, 1993] and cyclin B1 [Yuan et al., 2004] are key regulators of G1 and G2/M, respectively; and p21 is a cyclin-dependent kinase inhibitor that mediates both G1 and G2/M arrest [Harper et al., 1993; Agarwal et al., 1995; Bates et al., 1998; Ando et al., 2001]. Therefore, it is likely for cells expressing hepaCAM to undergo cell cycle arrest. Unexpectedly, there is no significant alteration in the cell cycle distribution of cells expressing hepaCAM. Such a phenomenon has also been observed in the tumor suppressor PTEN. Xu et al. [2002] have reported that the expression of PTEN in PTEN-null Jurkat T cell leukemia line inhibits cell proliferation without inducing cell cycle arrest. This finding is further supported by Seminario et al. [2003] who have shown that PTEN expression in Jurkat cells causes neither cell cycle arrest nor cell death. Instead, PTEN expression reduces Jurkat cell proliferation by slowing the progression of cells throughout the phases of the cell cycle, thereby resulting in a static cell cycle pattern. The delayed cell division of PTEN-transfected cells is accompanied by alterations in the expression of cell cycle regulators p27, cyclin A, cyclin B, cdk4, and cdc25A.

In conclusion, we have demonstrated that hepaCAM induces the human glioblastoma U373-MG cells to undergo differentiation. The degree of cell differentiation is dependent on the expression level of hepaCAM.

ACKNOWLEDGMENTS

We thank Dr. Celestial Yap (National University of Singapore, Singapore) for the kind gift of U373-MG cell line and Miss Asha Reka Das for her administrative assistance. This work was supported by National University of Singapore Academic Research Fund Grant (R-185-000-112-112 R-185-000-169-112) and Singapore Millennium Foundation Postdoctoral Fellowship Grant (to M.C.M).

REFERENCES

Adachi J, Ohbayashi K, Suzuki T, Sasaki T. 1999. Cell cycle arrest and astrocytic differentiation resulting from PTEN expression in glioma cells. J Neurosurg 91:822–830.

Agarwal ML, Agarwal A, Taylor WR, Stark GR. 1995. p53 controls both the G2/M and the G1 cell cycle checkpoints and mediates reversible growth arrest in human fibroblasts. Proc Natl Acad Sci USA 92:8493–8497.

Ando T, Kawabe T, Ohara H, Ducommun B, Itoh M, Okamoto T. 2001. Involvement of the interaction between p21 and proliferating cell nuclear antigen for the maintenance of G2/M arrest after DNA damage. J Biol Chem 276:42971–42977.

Barres BA. 1999. A new role for glia: Generation of neurons. Cell 97:667–670.

Bates S, Ryan KM, Phillips AC, Vousden KH. 1998. Cell cycle arrest and DNA endoreduplication following p21Waf1/Cip1 expression. Oncogene 17:1691–1703.

Bischoff J. 1997. Cell adhesion and angiogenesis. J Clin Invest 100:S37–S39.

Bleau AM, Holland EC. 2007. Trapping the mouse genome to hunt human alterations. Proc Natl Acad Sci USA 104:7737–7738.

Bovolenta P, Liem RK, Mason CA. 1984. Development of cerebellar astroglia: Transitions in form and cytoskeletal content. Dev Biol 102:248–259.

Cavenagh JD, Cahill MR, Kelsey SM. 1998. Adhesion molecules in clinical medicine. Crit Rev Clin Lab Sci 35:415–459.

Collins VP. 1998. Gliomas. Cancer Surv 32:37–51.

Dahl D. 1981. The vimentin-GFA protein transition in rat neuroglia cytoskeleton occurs at the time of myelination. J Neurosci Res 6:741–748.

DeAngelis LM. 2001. Brain tumors. N Engl J Med 344:114–123.

Favre-Kontula L, Rolland A, Bernasconi L, Karmirantzou M, Power C, Antonsson B, Boschert U. 2008. GlialCAM, an immunoglobulin-like cell adhesion molecule is expressed in glial cells of the central nervous system. Glia 56:633–645.

Ferreira A, Kosik KS. 1996. Accelerated neuronal differentiation induced by p53 suppression. J Cell Sci 109:1509–1516.

Gumbiner BM. 1996. Cell adhesion: The molecular basis of tissue architecture and morphogenesis. Cell 84:345–357.

Harper JW, Adami GR, Wei N, Keyomarsi K, Elledge SJ. 1993. The p21 Cdk-interacting protein Cip1 is a potent inhibitor of G1 cyclin-dependent kinases. Cell 75:805–816.

Hatten ME. 1984. Embryonic cerebellar astroglia in vitro. Brain Res 315:309–313.

Hatton JD, Hoi SU. 1993. In vitro differentiation inhibits the migration of cultured neonatal rat cortical astrocytes transplanted to the neonatal rat cerebrum. Int J Dev Neurosci 11:583–594.

Kim SO, Avraham S, Jiang S, Zagozdzon R, Fu Y, Avraham HK. 2004. Differential expression of Csk homologous kinase (CHK) in normal brain and brain tumors. Cancer 101:1018–1027.

Krex D, Klink B, Hartmann C, von Deimling A, Pietsch T, Simon M, Sabel M, Steinbach JP, Heese O, Reifenberger G, Weller M, Schackert G, German Glioma Network. 2007. Long-term survival with glioblastoma multiforme. Brain 130:2596–2606.

Leventhal PS, Feldman EL. 1996. Tyrosine phosphorylation and enhanced expression of paxillin during neuronal differentiation in vitro. J Biol Chem 271:5957–5960.

Levison SW, Goldman JE. 1993. Both oligodendrocytes and astrocytes develop from progenitors in the subventricular zone of postnatal rat forebrain. Neuron 10:201–212.

Li Y, Yin W, Wang X, Zhu W, Huang Y, Yan G. 2007. Cholera toxin induces malignant glioma cell differentiation via the PKA/CREB pathway. Proc Natl Acad Sci USA 104:13438–13443.

Menko AS, Boettiger D. 1987. Occupation of the extracellular matrix receptor, integrin, is a control point for myogenic differentiation. Cell 51: 51–57.

Mi H, Haeberle H, Barres BA. 2001. Induction of astrocyte differentiation by endothelial cells. J Neurosci 21:1538–1547.

Milasincic DJ, Dhawan J, Farmer SR. 1996. Anchorage-dependent control of muscle-specific gene expression in C2C12 mouse myoblasts. In Vitro Cell Dev Biol Anim 32:90–99.

Moh MC, Lee LH, Shen S. 2005a. Cloning and characterization of hepaCAM, a novel Ig-like cell adhesion molecule suppressed in human hepatocellular carcinoma. J Hepatol 42:833–841.

Moh MC, Zhang C, Luo C, Lee LH, Shen S. 2005b. Structural and functional analyses of a novel Ig-like cell adhesion molecule, hepaCAM, in the human breast carcinoma MCF7 cells. J Biol Chem 280:27366–27374.

Moh MC, Zhang T, Lee LH, Shen S. 2008. Expression of hepaCAM is downregulated in cancers and induces senescence-like growth arrest via a p53/p21-dependent pathway in human breast cancer cells. Carcinogenesis 29:2298–2305.

Nandan D, Clarke EP, Ball EH, Sanwal BD. 1990. Ethyl-3,4-dihydroxybenzoate inhibits myoblast differentiation: Evidence for an essential role of collagen. J Cell Biol 110:1673–1679.

Pringle NP, Yu WP, Howell M, Colvin JS, Ornitz DM, Richardson WD. 2003. Fgfr3 expression by astrocytes and their precursors: Evidence that astrocytes and oligodendrocytes originate in distinct neuroepithelial domains. Development 130:93–102.

Raff MC. 1996. Size control: The regulation of cell numbers in animal development. Cell 86:173–175.

Rasheed BK, Wiltshire RN, Bigner SH, Bigner DD. 1999. Molecular pathogenesis of malignant gliomas. Curr Opin Oncol 11:162–167.

Richardson A, Malik RK, Hildebrand JD, Parsons JT. 1997. Inhibition of cell spreading by expression of the C-terminal domain of focal adhesion kinase (FAK) is rescued by coexpression of Src or catalytically inactive FAK: A role for paxillin tyrosine phosphorylation. Mol Cell Biol 17:6906–6914.

Saitoh O, Periasamy M, Kan M, Matsuda R. 1992. cis-4-Hydroxy-L-proline and ethyl-3,4-dihydroxybenzoate prevent myogenesis of C2C12 muscle cells and block MyoD1 and myogenin expression. Exp Cell Res 200:70–76.

Sasaki T, Yamazaki K, Yamori T, Endo T. 2002. Inhibition of proliferation and induction of differentiation of glioma cells with Datura stramonium agglutinin. Br J Cancer 87:918–923.

Seminario MC, Precht P, Wersto RP, Gorospe M, Wange RL. 2003. PTEN expression in PTEN-null leukaemic T cell lines leads to reduced proliferation via slowed cell cycle progression. Oncogene 22:8195–8204.

Sherr CJ. 1993. Mammalian G_1 cyclins. Cell 73:1059–1065.

Xu Z, Stokoe D, Kane LP, Weiss A. 2002. The inducible expression of the tumor suppressor gene PTEN promotes apoptosis and decreases cell size by inhibiting the PI3K/Akt pathway in Jurkat T cells. Cell Growth Diff 13:285–296.

Yuan J, Yan R, Krämer A, Eckerdt F, Roller M, Kaufmann M, Strebhardt K. 2004. Cyclin B1 depletion inhibits proliferation and induces apoptosis in human tumor cells. Oncogene 23:5843–5852.